Niche displacement of human leukemic stem cells uniquely allows their competitive replacement with healthy HSPCs

Allison L. Boyd,[1,2,3] Clinton J.V. Campbell,[1,2,3] Claudia I. Hopkins,[1] Aline Fiebig-Comyn,[1] Jennifer Russell,[1] Jelena Ulemek,[1] Ronan Foley,[4] Brian Leber,[4] Anargyros Xenocostas,[5] Tony J. Collins,[1] and Mickie Bhatia[1,2,3]

[1]Stem Cell and Cancer Research Institute; [2]Department of Biochemistry and Biomedical Sciences; [3]Department of Chemistry and Chemical Biology; [4]Department of Pathology and Molecular Medicine, McMaster University, Hamilton, Ontario L8S 4L8, Canada
[5]Department of Medicine, Division of Hematology, Schulich School of Medicine, University of Western Ontario, London, Ontario N6A 3K7, Canada

Allogeneic hematopoietic stem cell (HSC) transplantation (HSCT) is currently the leading strategy to manage acute myeloid leukemia (AML). However, treatment-related morbidity limits the patient generalizability of HSCT use, and the survival of leukemic stem cells (LSCs) within protective areas of the bone marrow (BM) continues to lead to high relapse rates. Despite growing appreciation for the significance of the LSC microenvironment, it has remained unresolved whether LSCs preferentially situate within normal HSC niches or whether their niche requirements are more promiscuous. Here, we provide functional evidence that the spatial localization of phenotypically primitive human AML cells is restricted to niche elements shared with their normal counterparts, and that their intrinsic ability to initiate and retain occupancy of these niches can be rivaled by healthy hematopoietic stem and progenitor cells (HSPCs). When challenged in competitive BM repopulation assays, primary human leukemia-initiating cells (L-ICs) can be consistently outperformed by HSPCs for BM niche occupancy in a cell dose-dependent manner that ultimately compromises long-term L-IC renewal and subsequent leukemia-initiating capacity. The effectiveness of this approach could be demonstrated using cytokine-induced mobilization of established leukemia from the BM that facilitated the replacement of BM niches with transplanted HSPCs. These findings identify a functional vulnerability of primitive leukemia cells, and suggest that clinical development of these novel transplantation techniques should focus on the dissociation of L-IC–niche interactions to improve competitive replacement with healthy HSPCs during HSCT toward increased survival of patients.

CORRESPONDENCE
Mickie Bhatia:
mbhatia@mcmaster.ca

Abbreviations used: AML, acute myeloid leukemia; CB, cord blood; G-CSF, granulocyte colony-stimulating factor; HLA-A2, human leukocyte antigen A2; HSC, hematopoietic stem cell; HSCT, HSC transplantation; HSPCs, hematopoietic stem and progenitor cells; LBA, long bone area; Lin$^-$, lineage-depleted; L-IC, leukemia-initiating cell; LSC, leukemic stem cell; PB, peripheral blood; TBA, trabecular bone area; WBC, white blood cell.

Acute myeloid leukemia (AML) is a hematological neoplasm with a hierarchical cellular structure that is reminiscent of the normal hematopoietic system (Lapidot et al., 1994; Bonnet and Dick, 1997; Hope et al., 2004). Leukemic stem cells (LSCs), which sit at the top of this hierarchy, are particularly resistant to conventional therapeutic measures, contributing to minimum residual disease and ultimately causing patient relapse (Guzman et al., 2002). More recent insights suggest that the BM microenvironment plays a fundamental role in sheltering LSCs (Konopleva et al., 2002) and specifying their self-renewal properties (Raaijmakers et al., 2010; Schepers et al., 2013; Kode et al., 2014). Therefore, niche-targeted consolidation treatment strategies represent a promising mechanism to effectively compromise LSC self-renewal and eliminate minimum residual disease in AML. To inform novel therapeutic efforts toward this goal, it is necessary to develop a thorough understanding of LSC niche characteristics, in relation to those of hematopoietic stem cells (HSCs).

We have previously characterized geographical and molecular features that functionally define the HSC niche in vivo (Guezguez et al.,

The Rockefeller University Press $30.00
J. Exp. Med. 2014 Vol. 211 No. 10 1925-1935
www.jem.org/cgi/doi/10.1084/jem.20140131

The Journal of Experimental Medicine

2013), and in this study we extend these observations by reporting that LSC-enriched populations share an equivalent spatial and functional distribution in BM. Critically, we show that hematopoietic stem and progenitor cells (HSPCs) can rival leukemia-initiating cells (L-ICs) to populate vacant sites within the BM, which has been described to contain a limited number of saturable niches (Colvin et al., 2004; Czechowicz et al., 2007). We further demonstrate that in the context of established leukemic disease, it is necessary to dissociate leukemia-niche interactions before HSC transplantation (HSCT), to achieve competitive healthy reconstitution at the expense of LSC self-renewal.

RESULTS AND DISCUSSION

Spatial overlap exists between normal and leukemic stem cell–enriched populations in the BM

We have recently described anatomical boundaries within the BM that discretely define the functional localization of healthy HSCs (Guezguez et al., 2013). Relative to diaphyseal long bone areas (LBA), the cellular composition of trabecular bone areas (TBAs) provides a unique molecular microenvironment that preferentially accommodates self-renewing HSCs. Applying the same analytical techniques, we comparatively interrogated whether phenotypically immature leukemic cells share this nonuniform distribution in BM, using xenografted immunodeficient mice established as a reliable surrogate model. After transplantation with primary cells from AML patients or normal human donors, xenografted femurs were dissected along axial planes that delineate the borders between TBA and LBA regions (Fig. 1 A). Flow cytometric measurement of primitive $CD45^+CD34^+$ human hematopoietic cells indicated that, like their normal counterparts, immature leukemic cells were markedly more predominant in the cancellous TBA (Fig. 1, B and C). Longitudinal sectioning of frozen decalcified femurs further allowed more precise comparison of microanatomical distribution patterns of normal and leukemic hematopoiesis in situ. Using a high-resolution fluorescence-based imaging platform (Guezguez et al., 2013), human-specific $CD45^+CD34^+$ cells could be sensitively and accurately detected, paralleling our flow

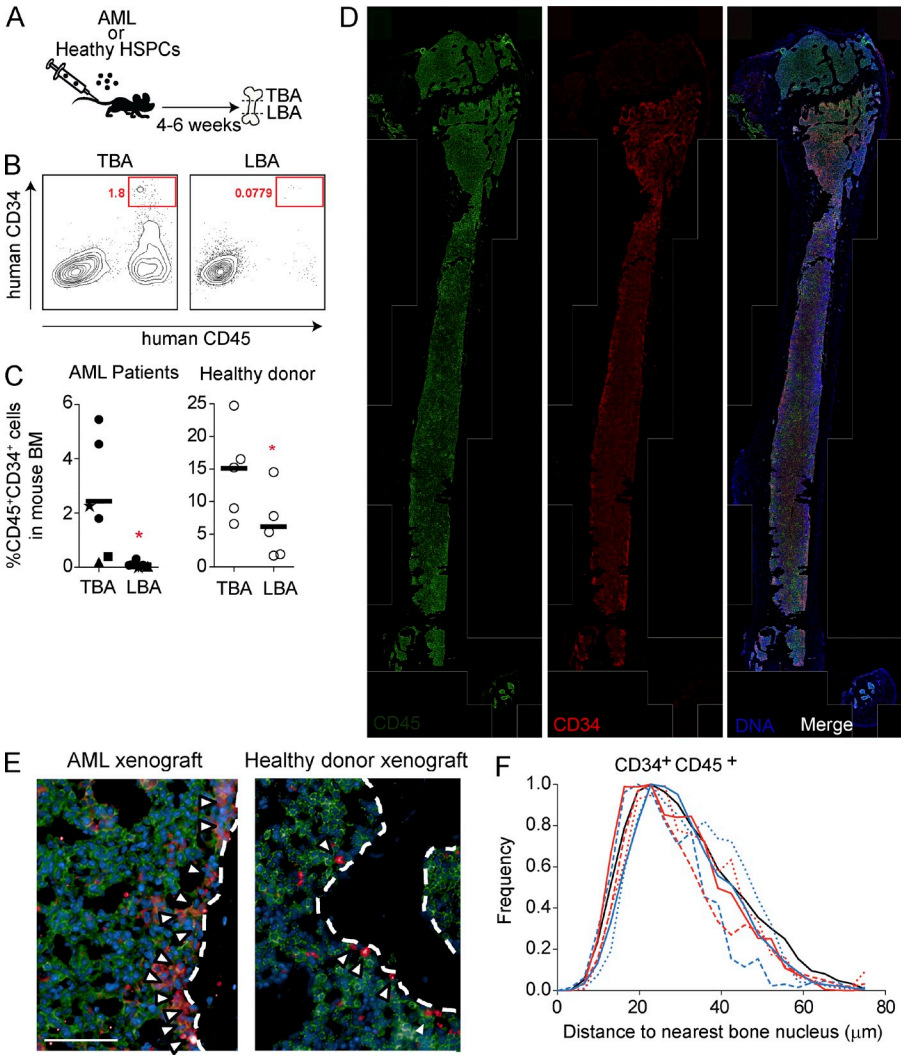

Figure 1. Healthy and leukemic human $CD34^+$ cells spatially overlap within the BM cavity. (A) Experimental design to study the location of healthy or leukemic human hematopoietic cells within the TBA and LBA of xenografted mouse femurs. (B) Representative flow cytometry plots showing human $CD45^+CD34^+$ AML cells within TBA and LBA regions. (C) Scatter plots showing the TBA- and LBA-specific frequencies of human $CD45^+CD34^+$ cells derived from AML patients or normal human donors. Each data point represents an individual mouse, and each symbol represents an independent primary human sample. *, $P < 0.05$, paired Student's *t* test. (D) Representative whole-bone section images of AML-engrafted mouse femurs immunostained with human-specific CD45 and CD34. Images have been montaged from 82 individual fields. Bar, 1 mm. (E) Representative high magnification images of AML or healthy donor-engrafted mouse femurs immunostained with human-specific CD45 and CD34. Dotted lines indicate the endosteal boundary. Bar, 50 µm. (F) Proximity distribution of healthy or leukemic human $CD45^+CD34^+$ cells relative to the nearest bone nucleus. Black line indicates the distribution of CB $CD45^+CD34^+$ cells (averaged across 4 replicates), and each colored line represents an independent AML-engrafted femur. Each color represents a different primary human AML sample. $P \geq 0.20$ when comparing AML $CD45^+CD34^+$ versus CB $CD45^+CD34^+$ distributions (Chi square).

cytometry analysis (Fig. S1, A and B). Enrichment of $CD34^+$ leukemic cells was evident along the surface area of the endosteum (Fig. 1, D and E), a geographical arrangement that has been previously described for both human and murine HSCs (Guezguez et al., 2013; Nombela-Arrieta et al., 2013). A customized quantitative localization analysis based on endosteal proximity (Fig. S1 C) showed that the spatial frequency distribution of $CD34^+$ AML cells is indistinguishable from that of normal HSPC donors (Fig. 1, E and F). This assessment extends observations of general associations of primitive AML cells with paratrabecular features (Ishikawa et al., 2007; Ninomiya et al., 2007; Fig. 1, B and C), and more specifically predicts that the regional distribution of normal and leukemic self-renewal niches are physically superimposed.

Healthy HSPCs can outcompete L-ICs to populate common functional BM sites

Although spatial profiling of phenotypically primitive cells provides compelling evidence that HSPCs and L-ICs share common BM niches, ultimately self-renewing cells are stringently defined based on their in vivo performance, requiring rigorous competitive transplantation assays to comprehensively address their predicted functional co-localization. To this end, human leukocyte antigen A2 (HLA-A2) served as a faithful antigen that allowed us to combine and track primary cells from genetically distinct human individuals within mixed chimeric xenografts (Guzman et al., 2002; Fig. S2). We initially performed competitive transplantation experiments between pairs of healthy cord blood (CB) donors, to first establish whether this cotransplantation xenograft model would accurately allow for the unbiased examination of BM niche repopulation dynamics (Fig. 2 A). Cell dose titration of co-injected donor cells revealed that relative initial $CD34^+$ cell content was strongly predictive of BM graft dominance (Fig. 2, B and C), reflecting clinical observations made in the context of human transplantation with mixed CB cells from two combined donors (Ballen et al., 2007). Furthermore, earlier transplantation provided a competitive repopulation advantage if donor cells were instead transplanted in a successive fashion (unpublished data), again recapitulating clinical reports (Ballen et al., 2007; Avery et al., 2011). In no instance did we observe evidence of immune recognition between donor cells (Yahata et al., 2004), as assured by the use of lineage-depleted (Lin^-) CB samples lacking $CD2^+$ T cells (Fig. 2 B), and the application of the NOD SCID recipient background, which precludes terminal maturation of immune competent lymphocytes (Shultz et al., 2005).

Using this clinically relevant system, we then cotransplanted constant cell numbers of AML with escalating doses of CB Lin^- cells to determine whether normal and leukemic repopulating cells can compete with each other to seed common BM niches (Fig. 2 D). All AML samples chosen for competitive repopulation experiments generated exclusively myeloid leukemic grafts (Fig. S3 A), and cotransplanted CB-HSPCs consistently gave rise to multilineage hematopoiesis (Fig. S3 B). Leukemic cell doses were chosen that would generate considerable levels of disease burden, to ensure that our model would accurately represent clinical situations of poor prognosis that would require HSCT therapy. Similar to our observations in paired CB donor–transplantation experiments, the proportions of AML patient-derived cells within the human grafts were consistently reduced by CB competition in a cell dose-dependent manner (Fig. 2, E and F). Remarkably, this translated into suppression of the absolute leukemic burden at higher CB Lin^- cell doses, unless the overall human reconstitution was low (AML Patient #1; Fig. 2, G and H). In this particular case of low human reconstitution, the presence of any competing CB cells was sufficient to compromise leukemic engraftment regardless of CB cell dose used (Fig. 2 I), and this observation was not unlike absolute engraftment profiles observed in double CB cotransplant experiments (Fig. 2 J). Overall, this demonstrates that normal and leukemic repopulating cells can compete dynamically to populate vacant BM niches and that L-ICs can be outcompeted by CB-HSPCs in a cell dose-dependent manner as long as niche availability is limiting. Our finding that L-ICs do not appear to have a superior affinity for niche repopulation was striking considering that primitive AML blasts have been reported to express elevated levels of antigens involved in adhesion and chemoattraction (De Waele et al., 1999; Jin et al., 2006).

When human cells from healthy/leukemic chimeras were serially transplanted into secondary recipients, we found that leukemic repopulation was equal to or less than that in primary recipient mice, whereas the self-renewal of AML-alone controls was uncompromised or elevated (Fig. 2, K and L). Therefore, the competitive pressure provided by co-injected HSPCs was apparently able to jeopardize L-IC fitness in a durable fashion. This would be an unlikely finding if L-ICs had the capacity to resist HSPC competition by relocation to alternative BM niches. When our model was instead adjusted to simulate the clinical context of preestablished leukemic disease followed by irradiation-conditioned CB Lin^- transplantation, leukemic engraftment was able to recur in secondary recipients, indicating less effective replacement of L-ICs (Fig. 2 M). This provides a model of leukemic relapse and complements our CB cotransplant studies, suggesting that equal competition for BM niches is compromised if leukemic engraftment is preestablished.

Mobilizing agents can displace leukemic cells from BM niches

We next reasoned that better capitalization of such unanticipated HSPC competitive properties would offer the most promising direction to improve therapeutic targeting of residual AML-LSCs during HSCT. Murine studies have suggested that small molecule or cytokine-induced mobilization of indigenous HSCs can effect dramatic niche exchange and HSC redistribution throughout BM (Verovskaya et al., 2014) and can also act as a preparative treatment to allow allogeneic HSC engraftment (Chen et al., 2006). We therefore sought to apply the same approach in a xenograft setting, to evaluate

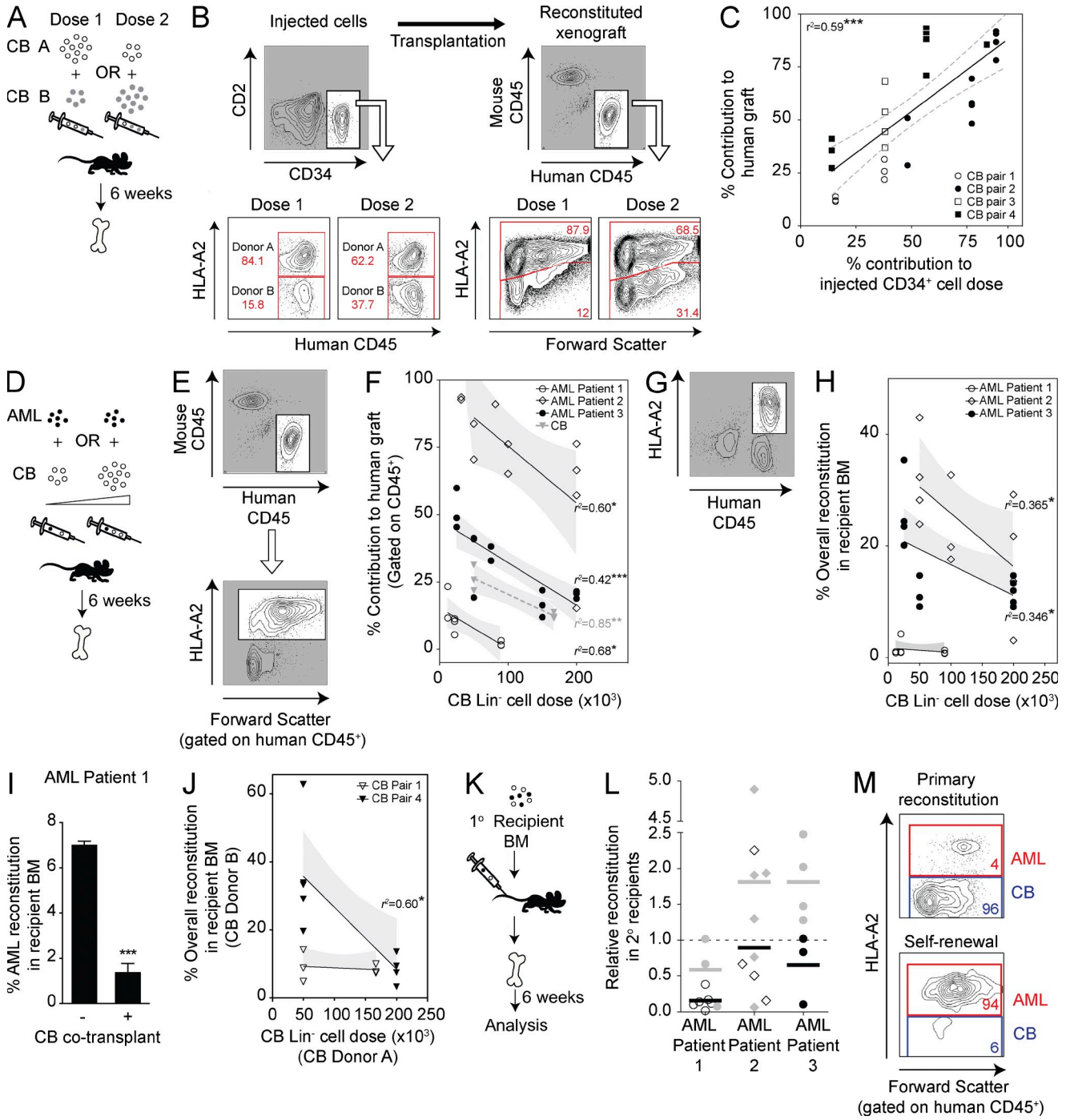

Figure 2. Cotransplantation of healthy HSPCs with AML MNCs can competitively reduce leukemic progression. (A) Experimental design to study competitive niche repopulation between HSPCs enriched from pairs of healthy human CB donors. (B) Gating strategy and representative flow cytometry plots showing relative donor cell proportions within human populations before and after co-injection into xenograft recipients. Top left plot shows that CD2⁺ T cells were absent from all injected Lin⁻ populations, precluding any immune reactions within the recipient mice. (C) Scatter plot of flow cytometry data showing that in mouse BM grafts, the relative donor CD45⁺ cell frequencies closely recapitulated their original proportions within injected CD34⁺ populations, consistently across four independent experiments using different CB donor pairs. Dotted lines represent 95% confidence intervals. Each data point represents an individual transplanted mouse. ***, $P < 0.0001$, linear regression. (D) Experimental design to study the effects of BM niche competition between healthy and leukemic human repopulating cells. AML cell numbers were kept constant with increasing dose titrations of CB Lin⁻ cells. (E) Example gating strategy to assess the relative reconstitution of primary AML samples in the presence of competing CB-HSPCs, expressed as a proportion of the total human graft. (F) Flow cytometry data showing that HSPC competition reduces the leukemic contribution to human grafts in a cell dose-dependent manner for all AML samples tested (three independent experiments). Cotransplantation of CB Pair #1 is also shown for comparison.

its therapeutic value to promote competition of transplanted HSPCs versus niche-occupant L-ICs. Initially, we assessed whether engrafted HSPCs and L-ICs would respond to mobilization treatment in similar ways based on their mutual dependence on CXCR4-CXCL12 for anchorage and retention in the BM (Peled et al., 1999; Petit et al., 2002; Tavor et al., 2004). Starting with CB-engrafted mice, we applied a mobilization regimen using two CXCR4-CXCL12 antagonists (granulocyte colony-stimulating factor; G-CSF and AMD3100), adapted from Petit et al. (2002) and Broxmeyer et al. (2005; Fig. 3 A). Consistent with previous studies (Nervi et al., 2009), we found that CXCR4 antagonism effectively mobilized xenografted human cells from the BM into the periphery within 1 h of treatment (Fig. 3 B). Although human hematopoietic cells were present in splenic isolates from both mobilized and control-treated mice, transplantation of these cells into secondary recipients revealed functional repopulating activity only among human cells that had been recovered from the spleens of mobilized mice (Fig. 3 C). This rigorous assessment of primitive functional characteristics is evidence that mobilization treatment successfully caused physical displacement of human long-term repopulating cells out of the BM, causing their redistribution into peripheral hematopoietic sites. We next applied the same treatment strategy to xenografts of primary human AML to establish whether leukemic cells could equally be displaced from the mouse BM (Fig. 3 D). Consistent with the niche similarities shared by normal and leukemic cells, mobilization treatment was also able to effect movement of human leukemic cells from the BM into the peripheral blood (PB) and spleens of diseased chimeric mice (Fig. 3 E). Recovered AML cells expressed appropriate tissue-specific and treatment-specific levels of CXCR4 (with the highest expression observed within the BM of mobilized mice; Petit et al., 2002; Fig. S4). Together, this suggests that the functional integrity of the CXCR4–SDF1 axis is intact and targetable in primitive AML cells.

This evidence that BM-resident leukemic cells can successfully be physically dislodged from their inhabited niches offers hope that leukemic mobilization could represent a mechanism to promote better competitive repopulation by HSPCs during therapeutic transplantation. Due to the inability of serial transplantation to discriminate between LSCs localized within specialized niches versus those transiting through nonniche BM space during mobilization, we explored the effects of mobilization on niche accessibility by challenging injected CB-HSPCs to home to the marrow after leukemic graft displacement. In our initial leukemia mobilization experiments, we found that within 1 d after treatment, the spatial configuration of the leukemic grafts had begun returning to a normal nonmobilized state, and that AML cells had completely reassumed their original tissue distribution by 1 wk after mobilization (unpublished data). We therefore reasoned that rapid infusion of competitive CB-HSPCs would be necessary after leukemic mobilization. 1 h after mobilization treatment of AML-engrafted mice, lipophilic dye-labeled CB Lin$^-$ cells were injected i.v. and the dissemination of these fluorescently labeled cells was assessed 1 d later (Fig. 3 F). Although a significant proportion of dye-labeled cells were localized to the spleen under both conditions at this time point, there was a modest reduction of these cells in premobilized mice (unpublished data). This was reflected by a twofold increase in CB Lin$^-$ cells homed to the BM (Fig. 3 G), suggesting that leukemic displacement led to increased niche availability. The observation of enhanced HSPC homing ability as a consequence of leukemic niche displacement supports our earlier interpretation that primitive normal and leukemic cells do share and compete for common microanatomical niches, and reinforces the prediction that leukemic mobilization can enhance competitive L-IC replacement by transplanted HSPCs.

Leukemic mobilization facilitates competitive reconstitution and leukemia elimination by transplanted HSPCs

Next, we evaluated the long-term effectiveness of preHSCT mobilization in the context of established leukemic disease by injecting large numbers of healthy CB-HSPCs after leukemic mobilization, to saturate the newly vacant BM niches (Fig. 4 A). Importantly, the injected CB Lin$^-$ cell doses were chosen such that the numbers of infused CD34$^+$ cells/kg body weight were representative of realistic cellular doses achievable in clinical human transplantation from adult HSPC sources (Körbling et al., 1995; Scheid et al., 1999; Table 1). Across three different patients,

Shaded areas represent 95% confidence intervals. Each data point represents an individual mouse. *, $P < 0.05$; **, $P < 0.01$; ***, $P < 0.001$, linear regression. (G) Example gating strategy to assess the absolute BM reconstitution levels of AML samples in the presence of CB-HSPC competition. (H) Flow cytometry data showing that absolute leukemic reconstitution is reduced by HSPC competition in a cell dose-dependent manner. Shaded areas represent 95% confidence intervals. Each data point represents an individual mouse. *, $P < 0.05$, linear regression. (I) Flow cytometry data showing that relative to control mice transplanted with AML cells alone, the total leukemic reconstitution of AML Patient #1 is reduced in the presence of competing HSPCs at all cell doses tested (single transplant $n = 2$, cotransplant $n = 8$). ***, $P < 0.0005$, unpaired Student's t test. (J) Flow cytometry data showing that absolute CB reconstitution levels are also influenced dose-dependently by competing CB donor cells only if human chimerism levels are high. Each data point represents an individual mouse. *, $P < 0.05$, linear regression. (K) Experimental design to study the effects of BM niche competition on the self-renewal ability of AML L-ICs by serial transplantation. (L) Flow cytometry data showing that in the presence of CB competition, leukemic chimerism after serial transplantation is either lower than or equal to leukemic reconstitution in primary recipients. Leukemic engraftment in secondary recipients was normalized to that of primary recipients (dotted line). Relative engraftment of control AML cells transplanted in the absence of CB is shown in gray. Each data point represents an individual mouse. (M) Representative flow cytometry plots gated on human CD45 show robust normal human reconstitution subsequent to therapeutic irradiation-conditioned CB Lin$^-$ transplantation of AML-engrafted mice (top), followed by AML recurrence after serial transplantation (bottom). Plots are representative of 6 mice that received irradiation-conditioned HSPC transplantation 3 wk after disease initiation, all of which had persistent leukemia after treatment.

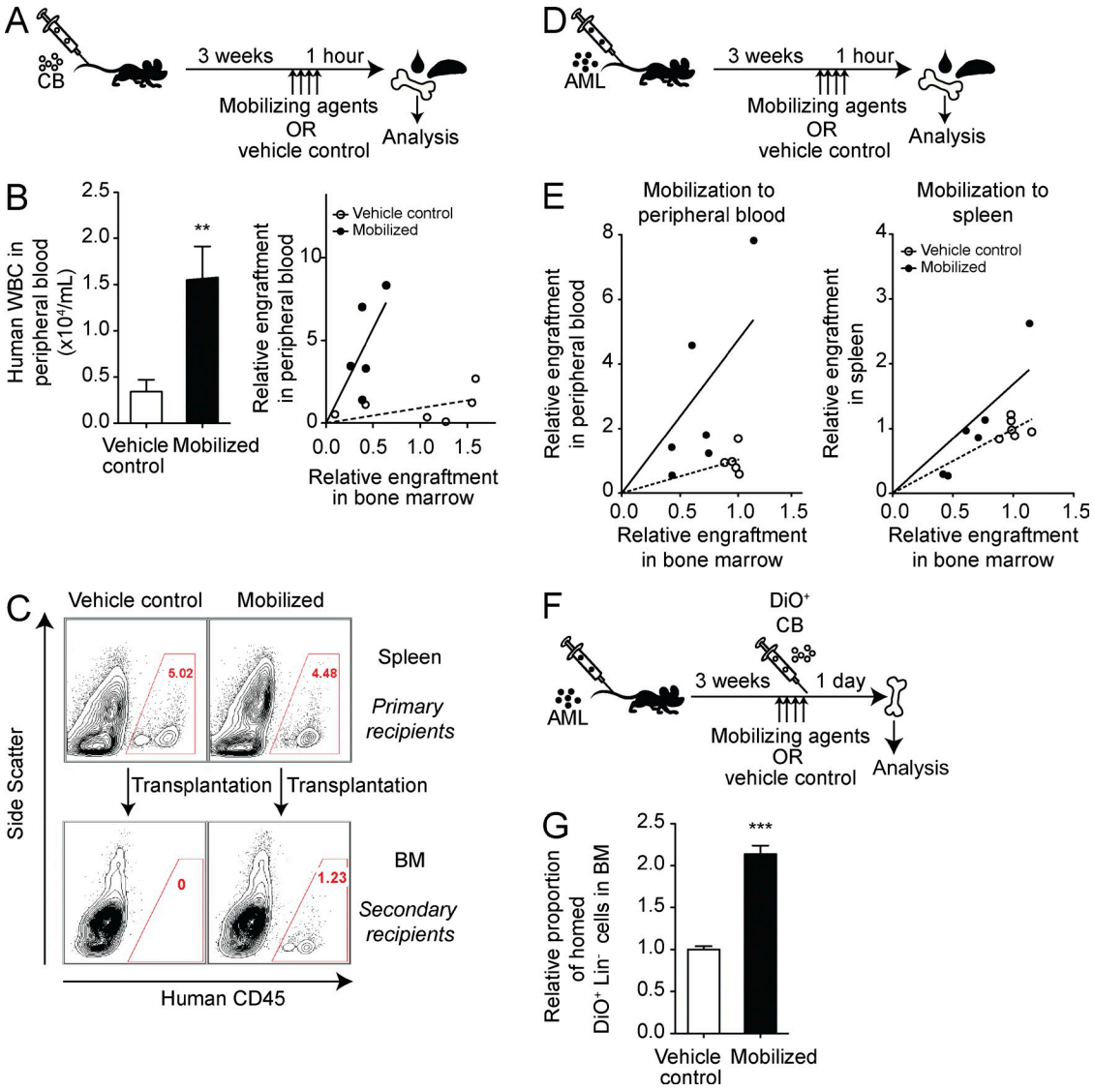

Figure 3. Mobilization treatment displaces normal and leukemic human repopulating cells from the xenograft BM niche, facilitating competitive homing by subsequent HSPC transplants. (A) Experimental design to investigate the effects of mobilization treatment on established human CB grafts. (B) Human WBC distribution 1 h after final treatment of CB xenografts with mobilization agents or vehicle (saline $n = 6$, mobilization $n = 5$). **, $P < 0.01$, unpaired Student's t test (bar graph). Each data point represents an individual mouse and slopes were significantly different (scatter plot; linear regression $P < 0.05$). (C) Representative flow cytometry plots show that human CD45⁺ cells can be detected in the spleens of xenografted mice 1 h after treatment with either vehicle or mobilization agents (top row). However, only splenic populations from mobilized mice possess repopulating activity, as measured by intrafemoral transplantation into secondary recipients (bottom row). Plots are representative of serial transplantation performed from spleens of 18 xenografted primary mice. (D) Experimental design to investigate the effects of mobilization agents on established human AML grafts. (E) Tissue distribution of human leukemic CD45⁺ cells 1 h after final treatment with mobilization agents or vehicle. Each data point represents an individual mouse. Slopes were significantly different, linear regression $P < 0.05$ (PB) and $P < 0.0005$ (spleen). (F) Experimental design to test whether mobilization of established human leukemic grafts can facilitate competitive niche replacement by subsequent HSPC transplants (CB Lin⁻ cells). (G) Relative frequency of DiO-labeled CB Lin⁻ cells homed to the BM of AML-engrafted mice after mobilization or vehicle treatment ($n = 3$ each). ***, $P < 0.005$, unpaired Student's t test.

mobilization preconditioning consistently ameliorated the ability of injected HSPCs to competitively reconstitute the leukemic xenograft microenvironment relative to nonmobilized controls (Fig. 4 B). In each case, this was accompanied by a statistically significant reduction in overall leukemic burden, as measured by overall leukemic cell frequencies in BM (Fig. 4 C) or total leukemia cell numbers per mouse (not depicted). Established healthy human grafts could be similarly suppressed by mobilization followed by transplantation with either normal or leukemic human cells (Fig. 4, D–G). This supports the notion that the temporal sequence of events is a fundamental determinant of competitive repopulation, and suggests that this is independent of the normal or leukemic nature of competing stem or progenitor cells. Critically, the superior therapeutic effects of mobilization

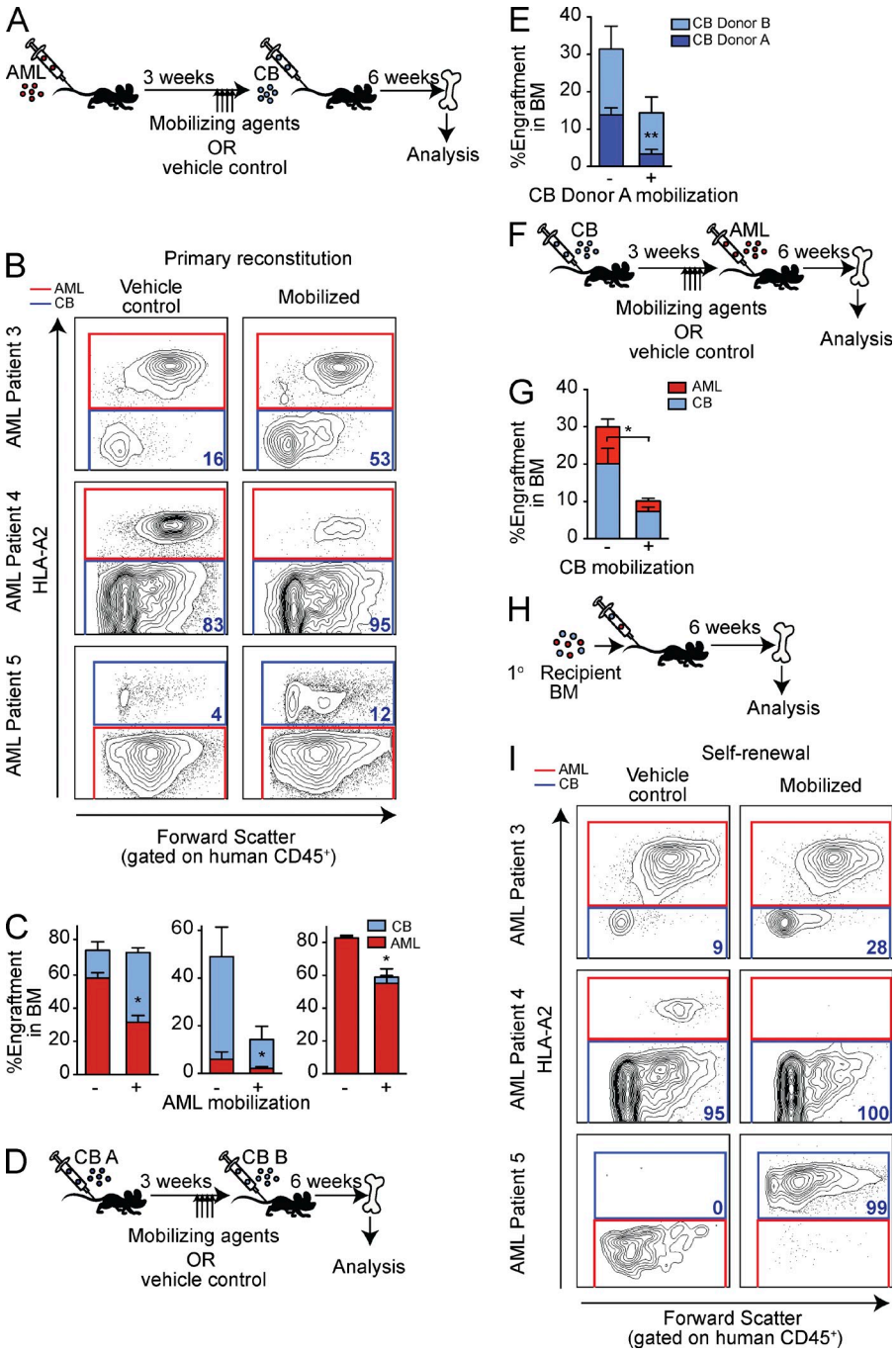

Figure 4. Leukemia mobilization facilitates competitive reconstitution by subsequent HSPC transplants at the expense of leukemic self-renewal. (A) Experimental design to test whether mobilization treatment of established AML grafts can facilitate competitive reconstitution by subsequent HSPC transplants (CB Lin$^-$ cells). (B) Representative flow cytometry plots gated on human CD45$^+$ populations. Gate frequencies indicate percent CB composition of human grafts (blue gates). (C) Summary of absolute human CB and leukemic engraftment levels showing that the total AML engraftment of three individual patients is reduced after mobilization-primed HSCT (n = 4–5 per group for each patient). Engraftment values are gated within all live events in BM. *, $P < 0.05$, unpaired Student's t test. (D) Experimental design to test whether mobilization treatment of established CB grafts can facilitate competitive reconstitution by subsequent healthy HSPC transplants. (E) Summary of absolute donor-specific engraftment levels showing that the chimerism levels of initial healthy donor grafts are reduced after mobilization-primed HSPC transplantation (n = 4 per group). Engraftment values are gated within all live events in BM. **, $P < 0.01$, unpaired Student's t test. (F) Experimental design to test whether mobilization treatment of established CB grafts can facilitate competitive reconstitution by subsequent AML transplantation. (G) Summary of absolute human CB and leukemic engraftment levels showing that the chimerism levels of initial healthy donor grafts are reduced after mobilization-primed AML transplantation (n = 4 per group). Engraftment values are gated within all live events in BM. *, $P < 0.05$, unpaired Student's t test. (H) Experimental design to assess the self-renewal potential of primary human AML grafts that were exposed to competitive repopulation by healthy HSPCs either with or without premobilization of leukemic cells. (I) Representative flow cytometry plots gated on human CD45 showing preferential self-renewal of HSPCs at the expense of AML L-ICs after mobilization-conditioned HSCT of leukemic mice. Gate frequencies indicate percent CB composition of human grafts (blue gates).

preconditioning persisted after each individual chimeric graft was serially transplanted into a single secondary recipient mouse (Fig. 4, H and I; and Table 2). In several cases, mobilization pretreatment involved complete elimination of L-IC repopulative capacity, with robust CB engraftment serving as a powerful positive internal control. This suggests that leukemic BM mobilization represents a promising HSCT preconditioning strategy, which can improve long-term management of leukemic disease.

Finally, to put our findings into a broader context for clinical application, we considered the predictive value of pretreatment disease levels toward therapeutic outcomes of mobilization HSCT. The robust therapeutic responses described for AML Patients #4 and #5 were associated with marginal frequencies of peripherally circulating leukemic blasts in primary mice at the time of treatment (Fig. 5 A), which provides an accurate surrogate representation of BM infiltration (Fig. 5 B). In contrast, mice treated under conditions of abundant

Table 1. CD34+ cell doses injected in mobilization-conditioned transplantation experiments, expressed per kg of recipient body weight

Sample	CD34+ cells × 10^6/kg body weight
AML Patient 3	19.4 ± 0.4
AML Patient 4	10.9 ± 0.2
AML Patient 5	15 ± 1

All doses are below reported clinically used values of 25.9 × 10^6 CD34+ cells/kg from adult HSPC sources (Scheid et al., 1999) and 40.1 × 10^6 CD34+ cells/kg (Körbling et al., 1995).

circulating blasts (Patient #6; Fig. 5 A) ultimately manifested aggressively disseminated disease with extramedullary leukemic burdens that exceeded the cellular capacity of the BM space (Fig. 5 C), despite mobilization-HSCT intervention (Fig. 5 D). This extreme example reinforces the principal suitability of mobilization-HSCT as a consolidation measure after cytoreduction (Rowe, 2009), and parallels clinical reports that poor disease-free survival is predicted by residual BM blast levels ≥ 30% at the time of conventional HSCT (Sierra et al., 2000; Kebriaei et al., 2005). Of fundamental significance, the therapeutic resistance of AML Patient #6 xenografts was accompanied by the notable absence of healthy CB self-renewal upon serial transplantation, despite successful healthy repopulation in primary recipients (Fig. 5 D). Therefore, transient repopulation by healthy hematopoietic progenitors is not sufficient to reverse leukemic progression, which instead requires durable niche population and engraftment by functionally defined HSCs (Fig. 4 I). These critical functional readouts provide evidence that HSCs rather than HPCs are most likely the direct LSC competitors, complementing recent insights implying functional similarities between HSC and LSC niches based on BM conditions that exacerbate murine AML (Krause et al., 2013) in a manner similar to niche-dependent HSC expansion (Calvi et al., 2003).

On the basis of in situ localization analysis and careful functional repopulation assays performed in vivo, we propose a model in which HSPCs and LSCs share and compete for common protective niches within the BM. Because the functional property of self-renewal is cell-extrinsically maintained (Guezguez et al., 2013), our finding of common regulatory niches between normal and leukemic stem cells presents a considerable barrier toward selective pharmacological targeting of LSC versus HSPC self-renewal. We instead suggest that novel approaches to cell-based therapy offer a more promising consolidation strategy to challenge LSC survival within the BM. To our knowledge, this represents the first demonstration that similar functional properties shared by LSCs and HSCs can be used as a therapeutic advantage in a preclinical transplantation model. Our study identifies a currently unexploited ability of HSPCs to rival L-ICs for BM niche territory, achievable by mobilization of resident L-ICs before healthy HSPC transplantation. This repositions transplanted HSPCs as powerful therapeutic effectors that can actively participate in LSC elimination, in contrast to their traditional reconstitutive role that is secondary to aggressive antileukemic therapy. The value in this novel mechanistic strategy is that LSC elimination can be accomplished without cytotoxic myeloablation, enhancing the safety and therapeutic index of HSCT through the repurposing of agents already known to be well-tolerated for patient administration (Bradley et al., 2012).

This potential for improved reduced-intensity conditioning could allow larger patient populations to be considered as HSCT candidates, and complements other toxicity-limiting strategies such as techniques that selectively deliver radiation targeted specifically to the BM, sparing other organs (Wong et al., 2006). The clinical application of leukemia mobilization for the purpose of HSCT is currently unprecedented, unlike the strategy of G-CSF–mediated chemotoxic sensitization (Saito et al., 2010), which has been subject to numerous patient trials over the past decade that have led to somewhat conflicting interpretations regarding efficacy (Estey et al., 1999; Löwenberg et al., 2003; Büchner et al., 2004). Based on the anticipated safety and the promising preclinical observations reported here, the testing and optimization of mobilization preconditioning as a new HSCT approach for AML patients is currently planned, including the evaluation of adult BM as a compatible HSPC source due to the greater CD34+ cell numbers that can be procured (Körbling et al., 1995; Scheid et al., 1999; Wagner et al., 2002). Additionally, although a single round of mobilization-primed transplantation provided an effective technique of disease suppression under conditions of considerable leukemic burden (AML Patients #3 and #5), further refinement of this procedure could involve repeated cycles of mobilization and HSPC infusion (Colvin et al., 2004; Bhattacharya et al., 2009) to capitalize on multiple windows of opportunity to competitively eliminate L-ICs. Ultimately, the use of mobilization pretreatment either alone or in conjunction

Table 2. Self-renewal analysis of human AML-CB cotransplants with or without mobilization treatment

	AML Patient 3		AML Patient 4		AML Patient 5	
Engraftment outcomes	Control	Mobilized	Control	Mobilized	Control	Mobilized
AML only	0/4	0/3	0/3	0/5	1/1	2/5
AML + CB	4/4	3/3	2/3	1/5	0/1	2/5
CB only	0/4	0/3	1/3	4/5	0/1	1/5
Total mice	7		8		6	

For each of three AML samples, it is indicated how many secondary transplant recipients were observed to have AML L-IC self-renewal, HSPC self-renewal, or both.

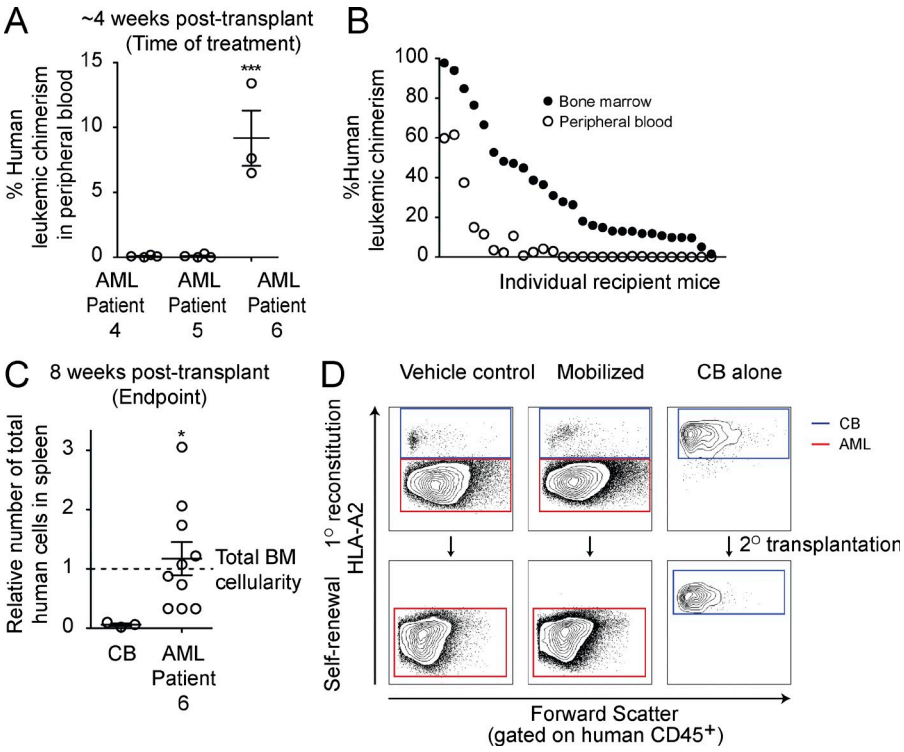

Figure 5. The leukemic burden at the time of mobilization–HSCT treatment influences therapeutic responses. (A) Circulating leukemic cell frequencies detected in PB at 3–4 wk post-disease initiation (when mobilization treatment and HSPC transplantation was performed). Each data point represents an individual mouse. ***, $P < 0.0005$, one-way ANOVA. (B) Matched PB and BM chimerism levels plotted from individual AML-engrafted mice analyzed at various time points after transplantation. Circulating blast levels increase dramatically once the leukemic infiltration of BM exceeds 50% chimerism. (C) The detection of substantial PB blast levels at 4 wk post-transplantation (shown in A) is related to an extremely aggressive course of disease culminating in 96 ± 1% leukemic chimerism in BM with extramedullary leukemic dissemination and dramatic splenomegaly by 8 wk post-disease initiation. The number of cells recovered from the spleens of mice transplanted with cells from AML Patient #6 approximated or even surpassed the cellularity from the entire BM (calculated according to Boggs, 1984). As a reference, the total abundance of human cells recovered from whole spleens is provided for CB-engrafted mice. *, $P < 0.05$, unpaired Student's *t* test. (D) Representative flow cytometry plots gated on human CD45 showing detectable healthy (HLA-A2$^+$) reconstitution in primary mice engrafted with AML Patient #6 cells and subsequently transplanted with healthy HSPCs. However, upon serial transplantation, HLA-A2$^+$ CB cells failed to self-renew, suggesting inadequate niche colonization. Cell-intrinsic CB-HSPC deficits are ruled out by HLA-A2$^+$ engraftment after serial transplantation of CB-alone controls. Plots are representative of 3–5 mice per group.

with low-intensity HSCT regimens offers a novel strategy toward the development of more tolerable AML transplantation therapy with superior eradication of residual disease.

MATERIALS AND METHODS

Primary human samples. Primary blasts were obtained from PB apheresis or BM aspirates of AML patients (Table S1), and healthy hematopoietic cells were isolated from CB samples. Informed consent was obtained from all sample donors in accordance with Research Ethics Board-approved protocols at McMaster University and the London Health Sciences Centre. Mononuclear cells were recovered by density gradient centrifugation (Ficoll-Paque Premium; GE Healthcare), and remaining red blood cells were lysed using ammonium chloride solution (StemCell Technologies). Lineage depletion of CB samples was performed using a commercially available kit (StemCell Technologies), according to the manufacturer's instructions.

Xenotransplant assays. NOD/Prkdc^{scid} and NOD/SCID/B2M^{null} mice were used as xenotransplantation recipients. Mice were bred in a barrier facility and all experimental protocols were approved by the Animal Care Council of McMaster University. Immunodeficient mice 6–10 wk of age were sublethally irradiated (350 rads, ^{137}Cs) 24 h before initial transplantation to induce and establish either healthy or leukemic human hematopoiesis (Lapidot et al., 1994; Bonnet and Dick, 1997). Pairs of human samples were selected based on disparate HLA-A2 expression, and were transplanted i.v. either separately or mixed together, according to established protocols (Sachlos et al., 2012; Guezguez et al., 2013). In some cases, mice received a second HLA-A2–mismatched human transplant after a period of 3 wk, as outlined in the text. 3–10 wk after original transplantation, mice were killed and cells from the BM and spleen were recovered by mechanical dissociation. After red blood cell lysis, species-specific CD45 antibodies were used to determine levels of human chimerism by flow cytometry. HLA-A2 targeted antibodies were then used to distinguish individual donor contributions to human grafts, and multilineage analysis involved antibodies directed toward CD33, CD19, CD34, and CXCR4 (BD). An LSRII flow cytometer (BD) was used for data acquisition, and all flow cytometry analysis was performed using FlowJo Software (version 9.3.2; Tree Star Inc.).

To assess self-renewal and evaluate the long-term persistence of L-ICs, normalized numbers of BM cells from individual engrafted mice were transplanted i.v. into single secondary recipients. In one experiment, cells recovered from the spleens of primary mice were transplanted intrafemorally into secondary recipients, by normalizing cell input based on organ volume. Engraftment of all secondary recipients was assessed 6–8 wk after transplantation using flow cytometry. The threshold used for human engraftment was 0.1% human CD45$^+$ chimerism within bone marrow (Notta et al., 2010).

Quantitative immunofluorescent microscopy. Whole femurs extracted from mice xenografted with healthy or leukemic hematopoietic cells were fixed overnight in 4% paraformaldehyde at 4°C, followed by overnight decalcification in formic acid (Immunocal; Decal). Femur specimens were subsequently snap frozen in OCT compound (Sakura) and sectioned at a 5-µm thickness with a cryostat microtome, using the CryoJane tape-transfer system (Leica). After blocking with 20% donkey serum (Jackson ImmunoResearch Laboratories) and mouse Fc receptor blocking (BD), slides were incubated with anti–human CD45 rat monoclonal antibody ab30446 and anti–human CD34 rabbit monoclonal antibody ab81289 (both 1:50 dilution; Abcam). Donkey-raised secondary antibodies conjugated to Alexa Fluor 488 or Alexa Fluor 647 fluorophores were used for the detection of immunopositive cells (Life Technologies). Fluorescent montage images of immunostained bone sections were acquired at 20× using an Operetta high content imaging system (Perkin Elmer), and assembled with Columbus analysis software (Perkin

Elmer). Quantitative proximity analysis relative to endosteal bone regions was performed as previously described (Guezguez et al., 2013), using customized scripts in Acapella (Perkin Elmer) and MATLAB (MathWorks) software. In brief, DAPI signal intensity was used to identify individual cell nuclei, and the fluorescence intensities of the remaining channels were then quantified for each nuclear and perinuclear region. Negative staining controls were used to set positive signal thresholds. Endosteal cells were defined as $CD45^-CD34^-$ cells in areas with low surrounding nuclear density and high perinuclear autofluorescence in the DAPI channel. X-Y spatial nuclei coordinates were then used to calculate the distance of each human $CD45^+CD34^+$ cell to the nearest endosteal-defined cell to generate spatial distribution histograms.

In vivo mobilization treatment of xenografts. After the establishment of human grafts, mice were injected subcutaneously with mobilization agents adapted according to published treatment schedules (Petit et al., 2002; Broxmeyer et al., 2005). This consisted of three consecutive days of subcutaneous G-CSF injections at 300 µg/kg, followed by a single SQ injection of AMD3100 (Sigma-Aldrich; 5 mg/kg) on the fourth day. Vehicle control animals were injected with equivalent volumes of saline. 1-2 h after the final injection, mice were either transplanted i.v. with CB Lin^- cells (or saline), or were killed for analysis of human cell tissue distribution.

Hematology. PB was collected from the mandibular vein of mice 1 h after treatment with mobilization agents or with vehicle. White blood cell (WBC) counts in peripheral circulation were evaluated using a Nexcelom Cellometer after acridine orange staining of diluted whole blood samples. Total WBC numbers were then expressed per unit volume of blood.

Homing assay. CB Lin^- cells were incubated with Vybrant DiO cell labeling solution (Life Technologies, Burlington, Canada), following manufacturer's instructions. 1.5×10^5 labeled Lin^- cells per mouse were transplanted i.v. into either mobilized or control-treated animals that had been engrafted with AML three weeks prior. 24 h after transplantation, the relative homing of labeled CB Lin^- cells was assessed in dissociated spleen and bone marrow cells by flow cytometry.

Statistical analysis. Data are represented as mean ± SEM (SEM). Unpaired two-tailed Student's *t* tests, one-way ANOVAs, or linear regressions were used for statistical comparisons, with the exception of the localization-based frequency distributions of normal versus leukemic $CD45^+CD34^+$ cells, which were statistically compared using χ^2 analysis. Statistical analyses were performed using Prism (version 5.0a; GraphPad) or MATLAB (MathWorks) software, and the criterion for statistical significance was $P < 0.05$.

Online supplemental material. Fig. S1 shows gating strategies to quantify primitive leukemic cells in xenografted mouse femurs. Fig. S2 shows that HLA-A2 mismatching provides a means to track hematopoietic cells from individual human donors transplanted into immunodeficient mice. Fig. S3 shows multilineage gating strategy for cotransplanted human AML and CB samples. Fig. S4 shows gating strategy to evaluate the influence of AML graft mobilization on CXCR4 expression. Table S1 lists clinical details of AML samples used. Online supplemental material is available at http://www.jem.org/cgi/content/full/jem.20140131/DC1.

We would like to acknowledge Jennifer Reid, Irene Tang, Marilyne Levadoux-Martin, and Monica Graham for their technical help, and thank Dr. Borhane Guezguez, Dr. Kristin Hope, Dr. Mio Nakanishi, and Lili Aslostovar for their valuable comments.

This work was supported by a research grant to M.B. from the Marta and Owen Boris Foundation and Canadian Cancer Society Research Institute. A.L.B. and C.J.V.C. were supported from graduate research scholarships from Ontario Graduate Scholarship and National Science and Engineering Research Council. A.L.B. is currently supported by Jans Graduate Scholarship in Stem Cell Research. M.B. is a Canada Research Chair in Stem Cell Biology and Regenerative Medicine.

The authors declare no competing financial interests.

Submitted: 21 January 2014
Accepted: 23 July 2014

REFERENCES

Avery, S., W. Shi, M. Lubin, A.M. Gonzales, G. Heller, H. Castro-Malaspina, S. Giralt, N.A. Kernan, A. Scaradavou, and J.N. Barker. 2011. Influence of infused cell dose and HLA match on engraftment after double-unit cord blood allografts. *Blood*. 117:3277–3285, quiz :3478. http://dx.doi.org/10.1182/blood-2010-08-300491

Ballen, K.K., T.R. Spitzer, B.Y. Yeap, S. McAfee, B.R. Dey, E. Attar, R. Haspel, G. Kao, D. Liney, E. Alyea, et al. 2007. Double unrelated reduced-intensity umbilical cord blood transplantation in adults. *Biol. Blood Marrow Transplant*. 13:82–89. http://dx.doi.org/10.1016/j.bbmt.2006.08.041

Bhattacharya, D., A. Czechowicz, A.G.L. Ooi, D.J. Rossi, D. Bryder, and I.L. Weissman. 2009. Niche recycling through division-independent egress of hematopoietic stem cells. *J. Exp. Med*. 206:2837–2850. http://dx.doi.org/10.1084/jem.20090778

Boggs, D.R. 1984. The total marrow mass of the mouse: a simplified method of measurement. *Am. J. Hematol*. 16:277–286. http://dx.doi.org/10.1002/ajh.2830160309

Bonnet, D., and J.E. Dick. 1997. Human acute myeloid leukemia is organized as a hierarchy that originates from a primitive hematopoietic cell. *Nat. Med*. 3:730–737. http://dx.doi.org/10.1038/nm0797-730

Bradley, A.M., A.M. Deal, L.W. Buie, and H. van Deventer. 2012. Neutropenia-associated outcomes in adults with acute myeloid leukemia receiving cytarabine consolidation chemotherapy with or without granulocyte colony-stimulating factor. *Pharmacotherapy*. 32:1070–1077. http://dx.doi.org/10.1002/phar.1150

Broxmeyer, H.E., C.M. Orschell, D.W. Clapp, G. Hangoc, S. Cooper, P.A. Plett, W.C. Liles, X. Li, B. Graham-Evans, T.B. Campbell, et al. 2005. Rapid mobilization of murine and human hematopoietic stem and progenitor cells with AMD3100, a CXCR4 antagonist. *J. Exp. Med*. 201:1307–1318. http://dx.doi.org/10.1084/jem.20041385

Büchner, T., W.E. Berdel, and W. Hiddemann. 2004. Priming with granulocyte colony-stimulating factor—relation to high-dose cytarabine in acute myeloid leukemia. *N. Engl. J. Med*. 350:2215–2216. http://dx.doi.org/10.1056/NEJM200405203502124

Calvi, L.M., G.B. Adams, K.W. Weibrecht, J.M. Weber, D.P. Olson, M.C. Knight, R.P. Martin, E. Schipani, P. Divieti, F.R. Bringhurst, et al. 2003. Osteoblastic cells regulate the haematopoietic stem cell niche. *Nature*. 425:841–846. http://dx.doi.org/10.1038/nature02040

Chen, J., A. Larochelle, S. Fricker, G. Bridger, C.E. Dunbar, and J.L. Abkowitz. 2006. Mobilization as a preparative regimen for hematopoietic stem cell transplantation. *Blood*. 107:3764–3771. http://dx.doi.org/10.1182/blood-2005-09-3593

Colvin, G.A., J.F. Lambert, M. Abedi, C.C. Hsieh, J.E. Carlson, F.M. Stewart, and P.J. Quesenberry. 2004. Murine marrow cellularity and the concept of stem cell competition: geographic and quantitative determinants in stem cell biology. *Leukemia*. 18:575–583. http://dx.doi.org/10.1038/sj.leu.2403268

Czechowicz, A., D. Kraft, I.L. Weissman, and D. Bhattacharya. 2007. Efficient transplantation via antibody-based clearance of hematopoietic stem cell niches. *Science*. 318:1296–1299. http://dx.doi.org/10.1126/science.1149726

De Waele, M., W. Renmans, K. Jochmans, R. Schots, P. Lacor, F. Trullemans, J. Otten, N. Balduck, K. Vander Gucht, B. Van Camp, and I. Van Riet. 1999. Different expression of adhesion molecules on CD34+ cells in AML and B-lineage ALL and their normal bone marrow counterparts. *Eur. J. Haematol*. 63:192–201. http://dx.doi.org/10.1111/j.1600-0609.1999.tb01767.x

Estey, E.H., P.F. Thall, S. Pierce, J. Cortes, M. Beran, H. Kantarjian, M.J. Keating, M. Andreeff, and E. Freireich. 1999. Randomized phase II study of fludarabine + cytosine arabinoside + idarubicin +/- all-trans retinoic acid +/- granulocyte colony-stimulating factor in poor prognosis newly diagnosed acute myeloid leukemia and myelodysplastic syndrome. *Blood*. 93:2478–2484.

Guezguez, B., C.J. Campbell, A.L. Boyd, F. Karanu, F.L. Casado, C. Di Cresce, T.J. Collins, Z. Shapovalova, A. Xenocostas, and M. Bhatia. 2013. Regional localization within the bone marrow influences the functional capacity of human HSCs. *Cell Stem Cell*. 13:175–189. http://dx.doi.org/10.1016/j.stem.2013.06.015

Guzman, M.L., C.F. Swiderski, D.S. Howard, B.A. Grimes, R.M. Rossi, S.J. Szilvassy, and C.T. Jordan. 2002. Preferential induction of apoptosis for primary human leukemic stem cells. *Proc. Natl. Acad. Sci. USA*. 99: 16220–16225. http://dx.doi.org/10.1073/pnas.252462599

Hope, K.J., L. Jin, and J.E. Dick. 2004. Acute myeloid leukemia originates from a hierarchy of leukemic stem cell classes that differ in self-renewal capacity. *Nat. Immunol*. 5:738–743. http://dx.doi.org/10.1038/ni1080

Ishikawa, F., S. Yoshida, Y. Saito, A. Hijikata, H. Kitamura, S. Tanaka, R. Nakamura, T. Tanaka, H. Tomiyama, N. Saito, et al. 2007. Chemotherapy-resistant human AML stem cells home to and engraft within the bone-marrow endosteal region. *Nat. Biotechnol*. 25:1315–1321. http://dx.doi.org/10.1038/nbt1350

Jin, L., K.J. Hope, Q. Zhai, F. Smadja-Joffe, and J.E. Dick. 2006. Targeting of CD44 eradicates human acute myeloid leukemic stem cells. *Nat. Med*. 12:1167–1174. http://dx.doi.org/10.1038/nm1483

Kebriaei, P., J. Kline, W. Stock, K. Kasza, M.M. Le Beau, R.A. Larson, and K. van Besien. 2005. Impact of disease burden at time of allogeneic stem cell transplantation in adults with acute myeloid leukemia and myelodysplastic syndromes. *Bone Marrow Transplant*. 35:965–970. http://dx.doi.org/10.1038/sj.bmt.1704938

Kode, A., J.S. Manavalan, I. Mosialou, G. Bhagat, C.V. Rathinam, N. Luo, H. Khiabanian, A. Lee, V.V. Murty, R. Friedman, et al. 2014. Leukaemogenesis induced by an activating β-catenin mutation in osteoblasts. *Nature*. 506:240–244. http://dx.doi.org/10.1038/nature12883

Konopleva, M., S. Konoplev, W. Hu, A.Y. Zaritskey, B.V. Afanasiev, and M. Andreeff. 2002. Stromal cells prevent apoptosis of AML cells by up-regulation of anti-apoptotic proteins. *Leukemia*. 16:1713–1724. http://dx.doi.org/10.1038/sj.leu.2402608

Körbling, M., Y.O. Huh, A. Durett, N. Mirza, P. Miller, H. Engel, P. Anderlini, K. van Besien, M. Andreeff, D. Przepiorka, et al. 1995. Allogeneic blood stem cell transplantation: peripheralization and yield of donor-derived primitive hematopoietic progenitor cells (CD34+ Thy-1dim) and lymphoid subsets, and possible predictors of engraftment and graft-versus-host disease. *Blood*. 86:2842–2848.

Krause, D.S., K. Fulzele, A. Catic, C.C. Sun, D. Dombkowski, M.P. Hurley, S. Lezeau, E. Attar, J.Y. Wu, H.Y. Lin, et al. 2013. Differential regulation of myeloid leukemias by the bone marrow microenvironment. *Nat. Med*. 19:1513–1517. http://dx.doi.org/10.1038/nm.3364

Lapidot, T., C. Sirard, J. Vormoor, B. Murdoch, T. Hoang, J. Caceres-Cortes, M. Minden, B. Paterson, M.A. Caligiuri, and J.E. Dick. 1994. A cell initiating human acute myeloid leukaemia after transplantation into SCID mice. *Nature*. 367:645–648. http://dx.doi.org/10.1038/367645a0

Löwenberg, B., W. van Putten, M. Theobald, J. Gmür, L. Verdonck, P. Sonneveld, M. Fey, H. Schouten, G. de Greef, A. Ferrant, et al. Dutch-Belgian Hemato-Oncology Cooperative GroupSwiss Group for Clinical Cancer Research. 2003. Effect of priming with granulocyte colony-stimulating factor on the outcome of chemotherapy for acute myeloid leukemia. *N. Engl. J. Med*. 349:743–752. http://dx.doi.org/10.1056/NEJMoa025406

Nervi, B., P. Ramirez, M.P. Rettig, G.L. Uy, M.S. Holt, J.K. Ritchey, J.L. Prior, D. Piwnica-Worms, G. Bridger, T.J. Ley, and J.F. DiPersio. 2009. Chemosensitization of acute myeloid leukemia (AML) following mobilization by the CXCR4 antagonist AMD3100. *Blood*. 113:6206–6214. http://dx.doi.org/10.1182/blood-2008-06-162123

Ninomiya, M., A. Abe, A. Katsumi, J. Xu, M. Ito, F. Arai, T. Suda, M. Ito, H. Kiyoi, T. Kinoshita, and T. Naoe. 2007. Homing, proliferation and survival sites of human leukemia cells in vivo in immunodeficient mice. *Leukemia*. 21:136–142. http://dx.doi.org/10.1038/sj.leu.2404432

Nombela-Arrieta, C., G. Pivarnik, B. Winkel, K.J. Canty, B. Harley, J.E. Mahoney, S.Y. Park, J. Lu, A. Protopopov, and L.E. Silberstein. 2013. Quantitative imaging of haematopoietic stem and progenitor cell localization and hypoxic status in the bone marrow microenvironment. *Nat. Cell Biol*. 15:533–543. http://dx.doi.org/10.1038/ncb2730

Notta, F., S. Doulatov, and J.E. Dick. 2010. Engraftment of human hematopoietic stem cells is more efficient in female NOD/SCID/IL-2Rgc-null recipients. *Blood*. 115:3704–3707. http://dx.doi.org/10.1182/blood-2009-10-249326

Peled, A., I. Petit, O. Kollet, M. Magid, T. Ponomaryov, T. Byk, A. Nagler, H. Ben-Hur, A. Many, L. Shultz, et al. 1999. Dependence of human stem cell engraftment and repopulation of NOD/SCID mice on CXCR4. *Science*. 283:845–848. http://dx.doi.org/10.1126/science.283.5403.845

Petit, I., M. Szyper-Kravitz, A. Nagler, M. Lahav, A. Peled, L. Habler, T. Ponomaryov, R.S. Taichman, F. Arenzana-Seisdedos, N. Fujii, et al. 2002. G-CSF induces stem cell mobilization by decreasing bone marrow SDF-1 and up-regulating CXCR4. *Nat. Immunol*. 3:687–694. http://dx.doi.org/10.1038/ni813

Raaijmakers, M.H., S. Mukherjee, S. Guo, S. Zhang, T. Kobayashi, J.A. Schoonmaker, B.L. Ebert, F. Al-Shahrour, R.P. Hasserjian, E.O. Scadden, et al. 2010. Bone progenitor dysfunction induces myelodysplasia and secondary leukaemia. *Nature*. 464:852–857.

Rowe, J.M. 2009. Optimal induction and post-remission therapy for AML in first remission. *Hematology Am. Soc. Hematol. Educ. Program*. 2009: 396–405.

Sachlos, E., R.M. Risueño, S. Laronde, Z. Shapovalova, J.-H. Lee, J. Russell, M. Malig, J.D. McNicol, A. Fiebig-Comyn, M. Graham, et al. 2012. Identification of drugs including a dopamine receptor antagonist that selectively target cancer stem cells. *Cell*. 149:1284–1297. http://dx.doi.org/10.1016/j.cell.2012.03.049

Saito, Y., N. Uchida, S. Tanaka, N. Suzuki, M. Tomizawa-Murasawa, A. Sone, Y. Najima, S. Takagi, Y. Aoki, A. Wake, et al. 2010. Induction of cell cycle entry eliminates human leukemia stem cells in a mouse model of AML. *Nat. Biotechnol*. 28:275–280.

Scheid, C., A. Draube, M. Reiser, A. Schulz, J. Chemnitz, S. Nelles, M. Fuchs, S. Winter, P.D. Wickramanayake, V. Diehl, and D. Söhngen. 1999. Using at least 5x10(6)/kg CD34+ cells for autologous stem cell transplantation significantly reduces febrile complications and use of antibiotics after transplantation. *Bone Marrow Transplant*. 23:1177–1181. http://dx.doi.org/10.1038/sj.bmt.1701748

Schepers, K., E.M. Pietras, D. Reynaud, J. Flach, M. Binnewies, T. Garg, A.J. Wagers, E.C. Hsiao, and E. Passegué. 2013. Myeloproliferative neoplasia remodels the endosteal bone marrow niche into a self-reinforcing leukemic niche. *Cell Stem Cell*. 13:285–299. http://dx.doi.org/10.1016/j.stem.2013.06.009

Shultz, L.D., B.L. Lyons, L.M. Burzenski, B. Gott, X. Chen, S. Chaleff, M. Kotb, S.D. Gillies, M. King, J. Mangada, et al. 2005. Human lymphoid and myeloid cell development in NOD/LtSz-scid IL2R gamma null mice engrafted with mobilized human hemopoietic stem cells. *J. Immunol*. 174:6477–6489. http://dx.doi.org/10.4049/jimmunol.174.10.6477

Sierra, J., B. Storer, J.A. Hansen, P.J. Martin, E.W. Petersdorf, A. Woolfrey, D. Matthews, J.E. Sanders, R. Storb, F.R. Appelbaum, and C. Anasetti. 2000. Unrelated donor marrow transplantation for acute myeloid leukemia: an update of the Seattle experience. *Bone Marrow Transplant*. 26:397–404. http://dx.doi.org/10.1038/sj.bmt.1702519

Tavor, S., I. Petit, S. Porozov, A. Avigdor, A. Dar, L. Leider-Trejo, N. Shemtov, V. Deutsch, E. Naparstek, A. Nagler, and T. Lapidot. 2004. CXCR4 regulates migration and development of human acute myelogenous leukemia stem cells in transplanted NOD/SCID mice. *Cancer Res*. 64:2817–2824. http://dx.doi.org/10.1158/0008-5472.CAN-03-3693

Verovskaya, E., M.J. Broekhuis, E. Zwart, E. Weersing, M. Ritsema, L.J. Bosman, T. van Poele, G. de Haan, and L.V. Bystrykh. 2014. Asymmetry in skeletal distribution of mouse hematopoietic stem cell clones and their equilibration by mobilizing cytokines. *J. Exp. Med*. 211:487–497. http://dx.doi.org/10.1084/jem.20131804

Wagner, J.E., J.N. Barker, T.E. DeFor, K.S. Baker, B.R. Blazar, C. Eide, A. Goldman, J. Kersey, W. Krivit, M.L. MacMillan, et al. 2002. Transplantation of unrelated donor umbilical cord blood in 102 patients with malignant and nonmalignant diseases: influence of CD34 cell dose and HLA disparity on treatment-related mortality and survival. *Blood*. 100:1611–1618.

Wong, J.Y., A. Liu, T. Schultheiss, L. Popplewell, A. Stein, J. Rosenthal, M. Essensten, S. Forman, and G. Somlo. 2006. Targeted total marrow irradiation using three-dimensional image-guided tomographic intensity-modulated radiation therapy: an alternative to standard total body irradiation. *Biol. Blood Marrow Transplant*. 12:306–315. http://dx.doi.org/10.1016/j.bbmt.2005.10.026

Yahata, T., K. Ando, H. Miyatake, T. Uno, T. Sato, M. Ito, S. Kato, and T. Hotta. 2004. Competitive repopulation assay of two gene-marked cord blood units in NOD/SCID/gammac(null) mice. *Mol. Ther*. 10:882–891. http://dx.doi.org/10.1016/j.ymthe.2004.07.029